11345 (1997); T. F. Franke, D. R. Kaplan, L. C. Cantley, A. Toker, *Science* **275**, 665 (1997); S. G. Kennedy *et al.*, *Genes Dev.* **11**, 701 (1997).
10. NIH 3T3 cells expressing activated oncogenic Akt were generated by viral infection of NIH 3T3 cells with a retrovirus expressing v-akt [T. Franke *et al.*, *Cell* **81**, 727 (1995)].
11. For labeling experiments, 4×10^5 cells in 35-mm dishes were cultured 1 day after transfection for 3 hours in 1 ml of phosphate-free Dulbecco's modified Eagle's medium containing 1 mCi/ml ortho-^{32}P (New England Nuclear) with or without 5% dialyzed serum. Cells were lysed in 20 mM Hepes, 1% Triton X-100, 0.5% NP-40, 150 mM NaCl, 20 mM NaF, 2 mM Na_3Va0_4, 10 mM β-glycerophosphate, and protease inhibitors. Lysates were precleared with protein A– or protein G–Sepharose with preimmune serum. Casp9 was immunoprecipitated with a monoclonal antibody (mAb) to FLAG or a polyclonal antibody to Casp9, washed, and analyzed by SDS–polyacrylamide gel electrophoresis (SDS-PAGE) and autoradiography or by phosphoimager analysis.
12. A rabbit antiserum to Casp9 was raised against purified recombinant His_6-active Casp9 and verified to be specific for Casp9 by immunoblotting experiments using a panel of recombinant caspases, including Casp3, Casp6, Casp7, Casp8, and Casp10.
13. D. R. Alessi and P. Cohen, *Curr. Opin. Genet. Dev.* **8**, 55 (1998).
14. H. Dudek *et al.*, *Science* **275**, 661 (1997).
15. 293T cells (10^7) were transiently transfected with 25 μg of pCMV6-myrAkt-HA or pcDNA (control) DNA. The activated form of Akt was generated by adding the NH_2-terminal Src myristoylation sequence to a pre-existing construct expressing Akt-HA in pCMV-6 (*19*). Cells were lysed 1 day later in 1.5 ml of 20 mM tris-HCl (pH 7.4), 140 mM NaCl, 1% NP-40, 10 mM NaF, 1 mM Na_3VaO_4, 1 mM EDTA, and protease inhibitors. After normalizing for protein concentration, lysates were precleared with protein G–Sepharose and preimmune serum for 1 hour and incubated at 4°C with 0.5 μg of rat high-affinity mAb to hemagglutinin (HA) (Boehringer-Mannheim), followed by addition of 10 μl of protein G–Sepharose (Pharmacia) for 1 hour. Alternatively, endogenous Akt was immunoprecipitated from 267 or 267-Ki-Ras cells with antibody to Akt (Santa Cruz Biotech), producing similar results (*4*). Immunoprecipitates were washed three times in lysis solution and two times in kinase solution [20 mM Hepes (pH 7.2), 10 mM $MgCl_2$, 10 mM $MnCl_2$, 1 mM DTT, and 3 μM ATP].
16. Q. Deveraux *et al.*, *EMBO J.* **17**, 2215 (1998).
17. S. M. Srinivasula *et al.*, *J. Biol. Chem.* **271**, 27099 (1996).
18. GST-Akt was expressed from a recombinant baculovirus in Sf9 cells with activated forms of PI3K to achieve kinase activation. GST-Akt was purified from Sf9 lysates by glutathione-Sepharose affinity chromatography.
19. To determine the effects of Akt-mediated phosphorylation on caspase activity, in vitro kinase reactions were performed as described (*17*), except that 0.1 mM ATP was substituted for [γ-^{32}P]ATP. Immobilized Akt was removed by centrifugation, and half the sample (20 μl) was incubated with 10 μM Ac-DEVD-pNA (Alexis) and 2 μM purified pro-Casp3 in a final volume of 0.1 ml of caspase buffer (50 mM Hepes, 1 mM EDTA, 0.1% CHAPS, 10% sucrose, and 5 mM dithiothreitol). Caspase activity was based on cleavage of the colorimetric substrate Ac-DEVD-pNA (*5*) and was normalized relative to Akt-untreated (mock) material. For Casp9 measurements, the addition of pro-Casp3 created a coupled Casp9 → Casp3 → DEVD-pNA reaction, because Casp9 does not efficiently cleave DEVD (*16*). Activity percent was measured and normalized to mock-treated samples. Anti-HA immune complexes prepared from control-transfected cells and immobilized GST control protein resulted in no significant alterations of caspase activity (*4*).
20. Pro-Casp9 and Pro-Casp9(C287A) cDNAs, as well as S183A and S196A mutants of these, were expressed with NH_2-terminal His_6-tags from pET23b in BL21 cells for production of processed Casp9 and unprocessed Casp9, respectively (*16*). Expression was induced with 0.2 mM isopropyl-β-D-thiogalactopyranoside at $OD_{600} \cong 0.6$ to 0.8 and ~25°C for 4 hours for the S183A mutant and for 1 hour for the S196A mutant. Proteins were affinity purified by Ni-chelate Sepharose (Pharmacia).
21. H. Kuwata, T. T. Yip, C. L. Yip, T. W. Hutchens, *Biochem. Biophys. Res. Commun.* **245**, 764 (1998).
22. For MS analysis, 1 pmol of a 1.826-kD synthetic peptide corresponding to a V8 fragment containing the Akt phosphorylation site in Casp9 was kinased in vitro or mock treated and spotted onto a SELDI chip (Ciphergen Biosystems, Palo Alto, CA) and imbedded with cinamininic acid matrix. Alternatively, 293T cells were transiently transfected with pCMV6-myrAktHA and pcDNA3-FLAG constructs encoding C287A mutants of either pro-Casp9 or pro-Casp9(S196A). Casp9 (wild type) and Casp9(S196A) were isolated by immunoprecipitation using antibody to FLAG, eluted from beads with glycine (pH 3.0), and digested with 0.05 U of V8 protease for 8 hours in 50 mM NH_4oAc (pH 4.0) at room temperature. The samples were then analyzed by SELDI as described above. An 80-dalton increase in mass indicated that the peptide fragment was phosphorylated.
23. Casp9 mutants were generated by site-directed polymerase chain reaction (PCR) mutagenesis from a human pro-Casp9 cDNA (V. Dixit) and subcloned into pcDNA3-FLAG, pCMV2-FLAG, or pET23b plasmids. The primer pairs used to generate the S183A and S196A mutants were 5′-CCGCACCCGCACTG-GCGCGAACATCGACTGTGAG-3′ plus 5′-CTCACAGT-CGATGTTCGCGCCAGTGCGGGTGCGG-3′; and 5′-CGGCGTCGCTTCTCCGCGCTGCATTTCCTGGTGG-3′ plus 5′-CCACCATGAAATGCAGCGCGGAGAAGCGACG-CCG-3′, respectively. PCR was performed for 16 cycles at 95°C for 30 s, 55°C for 1 min, and 68°C for 12 min. Twenty microliters of the reactions was digested with Dpn I (10 U) for subsequent subcloning into plasmids.
24. P. Li *et al.*, *Cell* **91**, 479 (1997); Q. L. Deveraux *et al.*, *EMBO J.* **17**, 2215 (1998).
25. L. del Peso, M. Gonzalez-Garcia, C. Page, R. Herrera, G. Nunez, *Science* **278**, 687 (1997); S. R. Datta *et al.*, *Cell* **91**, 231 (1997).
26. S. Srinivasula, M. Ahmad, T. Fernandes-Alnemri, E. Alnemri, *Mol. Cell* **1**, 949 (1998); X. Yang, H. Y. Chang, D. Baltimore, *ibid.*, p. 319.
27. J. Rotonda *et al.*, *Nature Struct. Biol.* **3**, 619 (1996).
28. J. S. Rhim *et al.*, *Proc. Natl. Acad. Sci. U.S.A.* **91**, 11874 (1994).
29. M. Krajewska *et al.*, *Cancer Res.* **57**, 1605 (1997).
30. M. H. Cardone *et al.*, *Cell* **90**, 315 (1997).
31. Q. Zhou *et al.*, *J. Biol. Chem.* **272**, 7797 (1997).
32. We thank J. Rhim for 267 Ki-Ras cells; T. G. Sambandan for mass spectroscopy advice; I. Tamm for IAP measurements; S. Kitada for help with cell lines; T. Bobo, A. Sinskey, and P. Sorger for support; and the members of the Reed lab for helpful discussions. This work was partially supported by a Biomeasure grant to M.C., a Department of Defense Breast Cancer grant to N.R., a Danish Natural Science Foundation grant (9600412) to H.R.S., and grants CA-69381 and CA-69515 from NIH and the National Cancer Institute.

13 August 1998; accepted 14 October 1998

Dual Requirement for Gephyrin in Glycine Receptor Clustering and Molybdoenzyme Activity

Guoping Feng,* Hartmut Tintrup,* Joachim Kirsch, Mia C. Nichol, Jochen Kuhse, Heinrich Betz, Joshua R. Sanes†

Glycine receptors are anchored at inhibitory chemical synapses by a cytoplasmic protein, gephyrin. Molecular cloning revealed the similarity of gephyrin to prokaryotic and invertebrate proteins essential for synthesizing a cofactor required for activity of molybdoenzymes. Gene targeting in mice showed that gephyrin is required both for synaptic clustering of glycine receptors in spinal cord and for molybdoenzyme activity in nonneural tissues. The mutant phenotype resembled that of humans with hereditary molybdenum cofactor deficiency and hyperekplexia (a failure of inhibitory neurotransmission), suggesting that gephyrin function may be impaired in both diseases.

The main inhibitory inputs to spinal cord and brain-stem motoneurons use glycine as a neurotransmitter (*1*). The α and β transmembrane subunits of glycine receptors (GlyRs) from spinal cord copurify with gephyrin, a 93-kD cytoplasmic protein (*2*). Gephyrin binds to the β subunit of the GlyR and to tubulin, thereby linking GlyRs to the cytoskeleton (*3*). This interaction appears to be important for the accumulation of GlyRs at synapses, because GlyRs are precisely colocalized with gephyrin at synapses in the brain and spinal cord, gephyrin aggregates GlyRs when coexpressed with them in heterologous cells, and attenuation of gephyrin synthesis with antisense oligonucleotides prevents clustering of GlyRs at synaptic sites on cultured spinal neurons (*4–6*). Molecular cloning of gephyrin (*7*) revealed unexpected similarity to three *Escherichia coli* proteins (moeA, moaB, and mog), a *Drosophila melanogaster* protein (cinnamon), and an *Arabidopsis thaliana* protein (cnx1), all of which are involved in the synthesis of a molybdenum-containing cofactor essential for the activity of molybdoenzymes (*8*). This conservation (Fig. 1A) suggested that genes of the

G. Feng, M. C. Nichol, J. R. Sanes, Department of Anatomy and Neurobiology, Washington University School of Medicine, St. Louis, MO 63110, USA. H. Tintrup, J. Kirsch, J. Kuhse, H. Betz, Department of Neurochemistry, Max-Planck Institute for Brain Research, Frankfurt 60528, Germany.

*These authors contributed equally to this work.
†To whom correspondence should be addressed. E-mail: sanesj@thalamus.wustl.edu

same bacterial operon may have been joined during evolution to form a multidomain protein that gained a novel function.

We disrupted the gephyrin gene by deleting exon 1 and upstream sequences responsible for initiating transcription and translation (*9, 10*). The mutant allele (Fig. 1B) was transferred to embryonic stem (ES) cells by electroporation, and two successfully targeted clones gave rise to germ-line chimeras (Fig. 1, C and D). Heterozygous offspring (geph$^{+/-}$) were phenotypically normal. Homozygous mutants (geph$^{-/-}$) were born in expected numbers, despite lacking detectable gephyrin mRNA (Fig. 1E) and protein (Fig. 1F). However, all geph$^{-/-}$ mice died within 1 day of birth. Thus, gephyrin was dispensable for embryonic development but essential for postnatal survival.

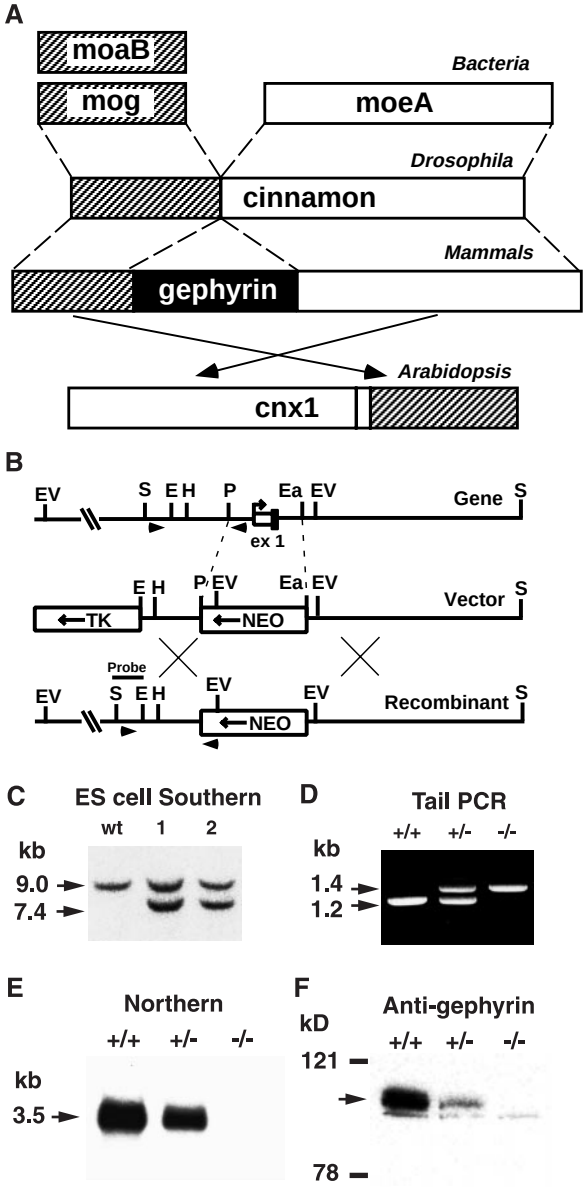

Fig. 1. Structure of gephyrin and generation of geph$^{-/-}$ mice. (**A**) Gephyrin shows similarity with proteins from *E. coli* (mog, moaB, and moeA), *Drosophila* (cinnamon), and *Arabidopsis* (cnx1) that have been implicated in molybdenum cofactor metabolism. MoaB/mog-like and moeA-like regions are indicated by hatched and open bars, respectively. (**B**) Targeting strategy. Wild-type *geph* gene (top), targeting vector (middle), and mutant locus (bottom) are shown. Sites of primers for polymerase chain reaction (PCR) genotyping (arrowheads) and external probe for Southern blot (DNA) analysis are indicated. E, Eco RI; Ea, Eag I; EV, Eco RV; H, Hind III; P, Pst I; S, Sac I; NEO, neomycin resistance gene; TK, thymidine kinase. (**C**) Southern blot analysis of wild-type and two successfully targeted ES cell clones. (**D**) PCR analysis of genomic DNA from wild-type (+/+), heterozygous (+/–), and homozygous (–/–) littermates. (**E**) Northern blot analysis of gephyrin mRNA from brain, using a full-length cDNA as probe. (**F**) Protein immunoblot analysis of gephyrin immunoreactivity from brain. The light band in all lanes represents nonspecific reactivity.

Geph$^{-/-}$ neonates appeared externally normal but failed to suckle and never produced the vocalizations characteristic of normal neonates. In response to mild tactile stimuli, control mice flailed their limbs, whereas geph$^{-/-}$ littermates assumed a rigid, hyperextended posture (Fig. 2, A and B). The mutants became increasingly hyperresponsive to tactile stimuli and exhibited apnea (difficulty breathing) by 12 hours after birth. These symptoms are consistent with impairment of inhibitory glycinergic inputs to motoneurons. To test this possibility, we stained spinal cord sections of geph$^{-/-}$ mice and littermate controls with antibodies to synaptic components (*11*). In controls, GlyRs and gephyrin are colocalized at inhibitory synapses on motoneuronal somata and primary dendrites (*4*). In homozygous mutants, synaptic boutons were numerous, but no gephyrin was detected, and GlyRs were diffusely distributed (Fig. 3A). Likewise, gephyrin and GlyRs were coclustered on subsets of neurons in the brainstem and hypothalamus of control neonates, but gephyrin was undetected and GlyRs were diffusely localized in geph$^{-/-}$ littermates (Fig. 3B). High levels of GlyR mRNA and protein persisted in geph$^{-/-}$ brains (Fig. 3, D and E), indicating that gephyrin was required for GlyR aggregation rather than GlyR synthesis. No difference was detected between mutants and controls in the size or distribution of glutamate receptor clusters, in the synaptic localization of their putative clustering proteins of the PSD-95/SAP-90 family (*12*), or in the overall morphology of the spinal cord and brain (Fig. 3, A and C). Thus, defects were specific for GlyRs.

The motor defects seen in geph$^{-/-}$ mice occurred earlier and were more severe than those observed in mutant mice that lack the GlyR α1 subunit or have reduced levels of the GlyR β subunit (*13*). This difference might be due to a more drastic reduction of synaptic GlyR levels in geph$^{-/-}$ mice, but the sequence similarity noted above (*7, 8*) raised the possibility that gephyrin might also be required for molybdenum metabolism. In fact, humans born with autosomal recessive molybdenum cofactor deficiency exhibit severe neurological defects that resemble those seen in geph$^{-/-}$ mice, such as hypertonicity, myoclonus, and difficulty in feeding (*14*). Molybdenum cofactor deficiency is diagnosed in humans by demonstrating coordinate loss of activity of two distinct molybde-

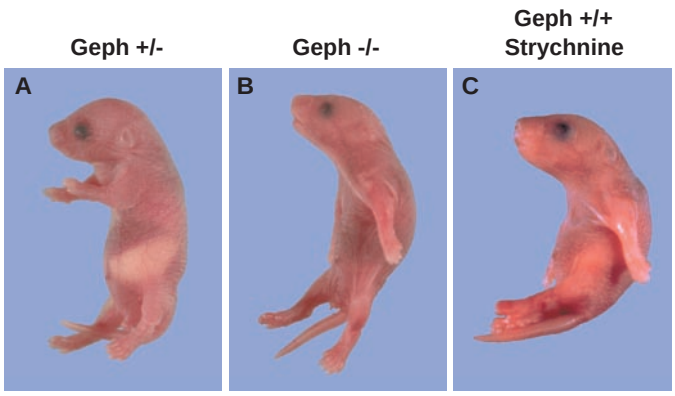

Fig. 2. Geph$^{+/-}$ (**A**), geph$^{-/-}$ (**B**), and geph$^{+/+}$ (**C**) mice approximately 8 hours after birth. Littermates in (A) and (B) were touched gently before photography, to show the rigid, hyperextended posture of geph$^{-/-}$ mice. Also note that the homozygote has no milk in its stomach. (C) Injection of a wild-type neonate with strychnine (1.4 μg/g of body weight) phenocopies the characteristic geph$^{-/-}$ posture.

num-containing enzymes, sulfite oxidase and xanthine dehydrogenase, which are ubiquitously expressed (*14*). We readily detected sulfite oxidase activity (*15*) in livers of control neonates, but not in livers of geph$^{-/-}$ mice (Fig. 4A). Xanthine dehydrogenase is not present in liver at birth even in controls, but is expressed in intestine. Xanthine dehydrogenase is also abundant in milk (*16*), so we avoided this source of contamination by assaying fetal intestine (*17*) and detected no activity in the homozygous mutants (Fig. 4B). As a control, we assayed the activity of an unrelated metabolic enzyme, lactate dehydrogenase, and the abundance of sulfite oxidase mRNA (*18*). Neither of these parameters differed among genotypes (Fig. 4, C and D). Thus, gephyrin appears to be essential for molybdenum cofactor biosynthesis in mice.

In view of these defects in molybdoenzyme activity, we considered the possibility that the neurological symptoms of geph$^{-/-}$ mice were secondary to their metabolic disorder rather than to disruption of glycinergic synapses. Two findings favor this possibility. First, patients with mutations in the sulfite oxidase gene are symptomatically similar to patients that lack molybdenum cofactor, suggesting that neurological defects in both groups result from sulfite toxicity (*19*). Second, glycinergic transmission may be excitatory rather than inhibitory in embryos (*20*). The developmental stage at which activation of GlyR becomes inhibitory is around birth in rats (*21*) but is unknown in mice. If it were postnatal, interference with glycinergic transmission might have a calming rather than a stimulatory effect on motor behavior, and the observed hyperresponsiveness of geph$^{-/-}$ mice could reflect sulfite toxicity. To address these issues, we injected neonatal mice with strychnine, a specific antagonist of GlyR (*21*). Like gephyrin mutants, strychnine-intoxicated neonates assumed a rigid, hyperextended posture in response to mild tactile stimuli (Fig. 2C). Thus, glycinergic transmission appeared to be predominantly inhibitory at birth, and blockade of glycinergic transmission in the absence of interference with molybdenum metabolism phenocopied the motor symptoms of gephyrin deficiency. Motor defects in geph$^{-/-}$ mice—and by implication, in molybdenum cofactor–deficient humans—may therefore result from both impaired inhibitory neurotransmission and impaired molybdoenzyme activity.

Our results demonstrate that gephyrin is essential for the synaptic clustering of GlyRs in vivo. Gephyrin may play a role at inhibitory synapses similar to that played by the clustering protein rapsyn at neuromuscular junctions (*22*). A second role of gephyrin is in synthesis of molybdenum cofactor. Homologous proteins have been described in other phyla (*8*), but no components of the molybdenum cofactor synthetic pathway have been identified in vertebrates. This peculiar pleiotropy raises four interesting possibilities. First, mutations in the gephyrin gene may underlie some cases of autosomal recessive human molybdenum cofactor deficiency. Second, some neurological symptoms now attributed to molybdoenzyme inactivity in humans may actually reflect a lack of receptor accumulation at inhibitory synapses. Third, although some cases of hyperekplexia (startle disease or stiff baby syndrome) are due to mutations in the GlyR (*23*), others might result from mutations of gephyrin, in

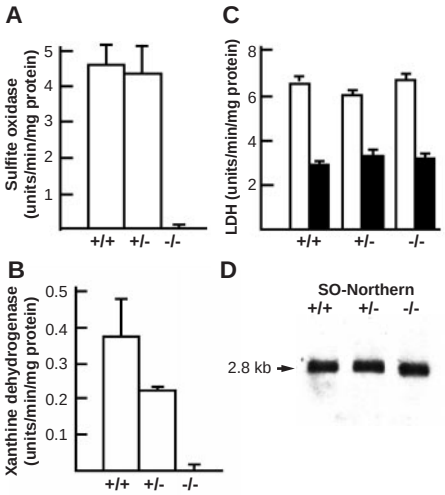

Fig. 4. Activities of two molybdoenzymes, sulfite oxidase (**A**) and xanthine dehydrogenase (**B**), and a control enzyme, lactic dehydrogenase (LDH) (**C**), in neonatal liver [(A) and open bars in (C)] and embryonic day-18 intestine [(B) and dark bars in (C)] of geph$^{-/-}$, geph$^{+/-}$, and geph$^{+/+}$ littermates. (**D**) Northern blot analysis of sulfite oxidase mRNA. Molybdoenzyme activities were undetected in geph$^{-/-}$ mice, but LDH levels and abundance of sulfite oxidase RNA did not vary significantly among genotypes.

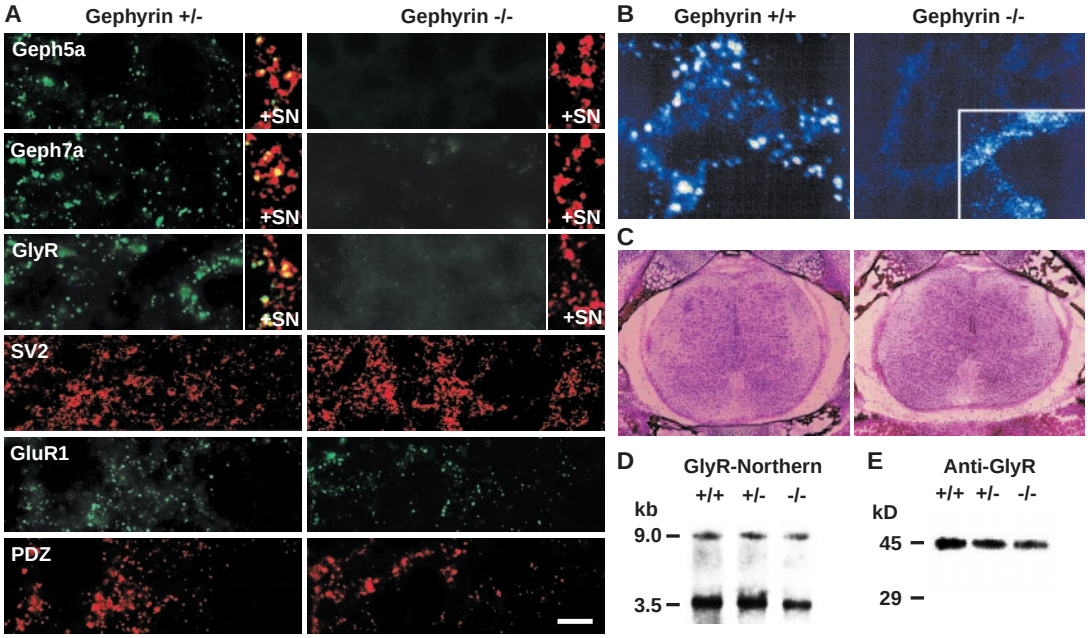

Fig. 3. Disrupted clustering of GlyRs in geph$^{-/-}$ mutant neonates. (**A**) Cryostat sections are shown of spinal cord stained with two antibodies to gephyrin that recognize distinct epitopes (5a and 7a), and with antibodies to the GlyR α1 subunit, the glutamate receptor GluR1 subunit, a conserved domain on several members of the PSD-95/SAP-90 family (PDZ), and the synaptic vesicle proteins SV2 and synaptophysin (SN). Gephyrin and GlyRs cocluster on motoneuronal somata and proximal dendrites in controls. Insets show localization of these proteins at synaptic sites by double labeling (green, gephyrin or GlyR; red, synaptophysin; yellow, overlap). Gephyrin is absent and GlyRs are diffusely distributed in mutants, but synapses are present. GluR1 and PSD-95–like proteins, shown in a double-labeled section, are clustered in both +/– and –/– mice. Bar, 10 μm. (**B**) Confocal images of GlyR immunoreactivity in hypothalamic neurons from +/+ and –/– mice. Inset shows a portion of the mutant neuron at increased gain, to demonstrate diffusely distributed GlyRs. (**C**) Geph$^{-/-}$ spinal cord exhibits normal overall morphology, revealed by staining with hematoxylin and eosin. (**D**) Northern blot analysis of GlyR α1 subunit mRNA in homozygous mutants and littermate controls. (**E**) Protein immunoblot analysis of GlyR immunoreactivity in mutant and controls.

which case some of the symptoms could reflect molybdenum insufficiency. Finally, activation or aggregation of GlyRs might modulate the ability of gephyrin to promote molybdopterin biosynthesis, thus resulting in a functional link between molybdoenzymes and inhibitory neurotransmission.

References and Notes

1. M. H. Aprison, in *Glycine Neurotransmission*, O. P. Ottoson and J. Storm-Mathisen, Eds. (Wiley, New York, 1990), pp. 1–24; P. Jonas, J. Bischofberger, J. Sandkühler, *Science* **281**, 419 (1998).
2. F. Pfeiffer, D. Graham, H. Betz, *J. Biol. Chem.* **257**, 9389 (1982).
3. G. Meyer, J. Kirsch, H. Betz, D. Langosch, *Neuron* **15**, 563 (1995); J. Kirsch *et al.*, *J. Biol. Chem.* **266**, 22242 (1991); J. Kirsch and H. Betz, *J. Neurosci.* **15**, 4148 (1995).
4. A. Triller, F. Cluzeaud, F. Pfeiffer, H. Betz, H. Korn, *J. Cell Biol.* **101**, 683 (1985); J. Kirsch and H. Betz, *Brain Res.* **621**, 301 (1993); A. J. Todd, R. C. Spike, D. Chong, M. Neilson, *Eur. J. Neurosci.* **7**, 1 (1995).
5. J. Kirsch, J. Kuhse, H. Betz, *Mol. Cell. Neurosci.* **6**, 450 (1995); J. Kirsch, I. Wolters, A. Triller, H. Betz, *Nature* **366**, 745 (1993).
6. J. Kirsch, G. Meyer, H. Betz, *Mol. Cell. Neurosci.* **8**, 93 (1996); C. Bechade and A. Triller, *Semin. Cell Dev. Biol.* **7**, 717 (1996).
7. P. Prior *et al.*, *Neuron* **8**, 1161 (1992).
8. K. V. Rajagopalan, *Biochem. Soc. Trans.* **25**, 757 (1997); K. P. Kamdar *et al.*, *ibid.*, p. 778; B. Stallmeyer, A. Nerlich, J. Schiemann, H. Brinkmann, R. R. Mendel, *Plant J.* **8**, 751 (1995).
9. M. Ramming, H. Betz, J. Kirsch, *FEBS Lett.* **405**, 137 (1997).
10. The targeting vector contained a 5-kb Eco RI/Sac I genomic fragment in which a phosphoglycerate kinase–neo cassette replaced a Pst I/Eag I fragment that encoded the putative promoter region of the murine gephyrin gene as well as the first exon, which included the initiator methionine (*9*). The construct was transfected into R1 ES cells [A. Nagy, J. Rossant, R. Nagy, W. Abramow-Newerly, J. C. Roder, *Proc. Natl. Acad. Sci. U.S.A.* **90**, 8424 (1993)], and 20 of 200 clones screened were identified as homologous recombinants. Homozygotes derived from two independently derived ES cell clones showed identical phenotypes. For Southern (DNA) analysis, a 0.6-kb probe external to the short arm (Fig. 1B) was hybridized to Eco RV–digested genomic DNA. For Northern analysis, 10-μg aliquots of polyadenylated RNA from brain were separated in a 1% agarose gel, and a blot was probed successively with cDNAs encoding mouse gephyrin, sulfite oxidase, or GlyR α1 subunit. For Western analysis, brain protein extracts were fractionated on 6% or 10% SDS polyacrylamide gels, and immunoblots were probed with mouse monoclonal antibodies directed against the COOH-terminus of gephyrin (Transduction Labs) or GlyR subunits [monoclonal antibody (mAb) 4a; (*24*)].
11. Spinal cords and brains were cross-sectioned at 7 μm in a cryostat. Sections were fixed with 4% paraformaldehyde and stained with antibodies specific for GlyR α1 subunit [mAb 2b; (*24*)], gephyrin [mAbs 5a and 7a; (*24*)], SV2 (gift of K. Buckley, Harvard University), the PSD-95/SAP-90 family (Upstate Biotechnology), the glutamate receptor GluR1 subunit (Upstate Biotechnology), or synaptophysin (gift of A. Czernik, Rockefeller University). Other sections were stained with hematoxylin and eosin.
12. M. Sheng and M. Wyszynski, *Bioessays* **19**, 847 (1997).
13. E. S. Simon, *Mov. Disord.* **12**, 221 (1997).
14. J. L. Johnson and S. K. Wadman, in *The Metabolic Basis of Inherited Diseases*, C. R. Scrivner, A. L. Beaudef, W. S. Sly, D. Valle, Eds. (McGraw-Hill, New York, 1995), pp. 2271–2283
15. For sulfite oxidase assay, livers were homogenized and centrifuged at 16,000*g* for 20 min. Supernatants were desalted on Sephadex G-25 (Pharmacia). Activity in the flow-through was determined as described [J. L. Johnson *et al.*, *J. Inherit. Metab. Dis.* **14**, 932 (1991)].
16. M. Nakamura and I. Yamazaki, *J. Biochem.* **92**, 1279 (1972).
17. Xanthine dehydrogenase assay was modified from D. A. Parks, T. K. Williams, and J. S. Beckman [*Am. J. Physiol.* **254** 768 (1988)]. Intestines were homogenized in 50 mM potassium phosphate (pH 7.0), 10 mM dithiothreitol, 1 mM phenylmethylsulfonyl fluoride, and 0.1 mM EDTA. After centrifugation at 16,000*g* for 20 min, 200-μl aliquots of supernatant were incubated with 100 μl of 500 μM nicotinamide adenine dinucleotide, 100 μl of 50 μM xanthine, and 600 μl of 50 mM potassium phosphate (pH 7.8). Formation of uric acid from xanthine was monitored at 295 nm wavelength in the presence or absence of 5 μM allopurinol, an inhibitor of xanthine dehydrogenase [R. W. E. Watts, J. E. M. Watts, J. E. Seegmiller, *J. Lab. Clin. Med.* **66**, 688 (1965)].
18. Lactate dehydrogenase activity was determined as described [A. Yoshida and E. Freese, *Methods Enzymol.* **41**, 304 (1975)]. Protein was assayed with the Bradford reagent (Bio-Rad).
19. C. A. Rupar *et al.*, *Neuropediatrics* **27**, 299 (1996).
20. H. Nishimaru, M. Iizuka, S. Ozaki, N. Kudo, *J. Physiol. (London)* **497**, 131 (1996).
21. W.-L. Wu, L. Ziskind-Conhaim, M. A. Sweet, *J. Neurosci.* **12**, 3935 (1992).
22. M. Gautam *et al.*, *Nature* **377**, 232 (1995); M. Gautum *et al.*, *Cell* **85**, 525 (1996); T. M. DeChiara *et al.*, *ibid.*, p. 501; J. R. Sanes and J. W. Lichtman, *Annu. Rev. Neurosci.*, in press.
23. W. Brune *et al.*, *Am. J. Hum. Genet.* **58**, 959 (1996); M. Andrew and M. J. Owen, *Br. J. Psychiatry* **170**, 106 (1997).
24. F. Pfeiffer, R. Simler, G. Grenningloh, H. Betz, *Proc. Natl. Acad. Sci. U.S.A.* **81**, 7224 (1984).

25. Supported by grants from NIH (J.R.S.), the Jane Coffin Childs Memorial Fund for Medical Research (G.F.), the McKnight Foundation (J.R.S.) the Deutsche Forschungsgemeinschaft, BMBF, and Fonds der Chemischen Industrie (H.B.). We thank I. Bartuik, C. Borgmeyer, J. Cunningham, J. Gross, and S. Weng for assistance. We dedicate this paper to the memory of Rolf Westkamp.

20 August 1998; accepted 25 September 1998

Structure of Human Methionine Aminopeptidase-2 Complexed with Fumagillin

Shenping Liu, Joanne Widom, Christopher W. Kemp, Craig M. Crews, Jon Clardy*

The fungal metabolite fumagillin suppresses the formation of new blood vessels, and a fumagillin analog is currently in clinical trials as an anticancer agent. The molecular target of fumagillin is methionine aminopeptidase-2 (MetAP-2). A 1.8 Å resolution crystal structure of free and inhibited human MetAP-2 shows a covalent bond formed between a reactive epoxide of fumagillin and histidine-231 in the active site of MetAP-2. Extensive hydrophobic and water-mediated polar interactions with other parts of fumagillin provide additional affinity. Fumagillin-based drugs inhibit MetAP-2 but not MetAP-1, and the three-dimensional structure also indicates the likely determinants of this specificity. The structural basis for fumagillin's potency and specificity forms the starting point for structure-based drug design.

Angiogenesis, the growth of new blood vessels, is a pathological determinant in tumor progression, diabetic retinopathy, and rheumatoid arthritis (*1*). The serendipitous discovery that fumagillin, a fungal metabolite, potently inhibits angiogenesis initiated the systematic development of small molecule angiogenesis inhibitors (*2, 3*) (Fig. 1). One semisynthetic derivative of fumagillin, TNP-470, is in clinical trials as an anticancer agent (Fig. 1) (*3, 4*). Fumagillin-based affinity reagents identified MetAP-2 as the specific cellular target of fumagillin, and this specificity was confirmed with genetically altered yeast strains (*5, 6*). The correlation between the antiproliferative activity of several fumagillin analogs with their ability to inhibit MetAP-2 activity in vitro suggests that MetAP-2 is the physiologically relevant target of fumagillin-based therapeutic agents (*6*). This suggestion is strengthened by a recent report that human endothelial cells are especially sensitive to fumagillin and that proliferation of these cells can be blocked by human MetAP-2 antisense oligonucleotides (*7*). MetAPs, which

S. Liu, J. Widom, J. Clardy, Department of Chemistry and Chemical Biology, Baker Laboratory, Cornell University, Ithaca, NY 14853–1301, USA. C. W. Kemp, Kemp Biotechnologies, Incorporated, Frederick, MD 21704, USA. C. M. Crews, Department of Molecular, Cellular, and Developmental Biology, Kline Biology Tower, Yale University, New Haven, CT 06520–8103, USA.

*To whom correspondence should be addressed. E-mail: jcc12@cornell.edu

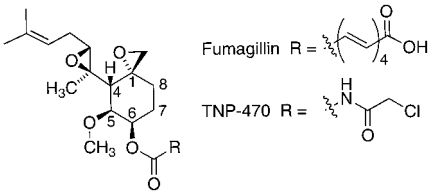

Fig. 1. The chemical structure of fumagillin and TNP-470.

Science

Dual Requirement for Gephyrin in Glycine Receptor Clustering and Molybdoenzyme Activity

Guoping Feng, Hartmut Tintrup, Joachim Kirsch, Mia C. Nichol, Jochen Kuhse, Heinrich Betz and Joshua R. Sanes

Science **282** (5392), 1321-1324.
DOI: 10.1126/science.282.5392.1321